Real-Time Control of Sheet Stability During Forming

D. E. Hardt
Leaders for Manufacturing Professor of Mechanical Engineering.

R. C. Fenn
Research Assistant.

Laboratory for Manufacturing and Productivity,
Massachusetts Institute of Technology,
Cambridge, MA 02139

During the stamping of complex three-dimensional sheet metal parts, the in-plane compressive stresses created often lead to failure by buckling. These are typically suppressed by binding the material at the periphery to provide a tensile bias. In practice, these biases are difficult to determine, and must be addressed with a combination of a priori analysis and die-making skill. Even then, in-process variations will cause parts to begin failing by tearing or buckling as friction, material, or geometric changes occur. In this paper two methods are presented for controlling the blankholder force in-process to ensure optimal forming conditions at all times. This is effectively a signature-following method based on replicating either a previously determined optimal forming-punch force trajectory or a normalized average thickness trajectory. The method is implemented using closed-loop control of these quantities, and subjected to experiments where various disturbances are presented. Previously reported results for axisymmetric shapes indicated the ability to eliminate the effect of uncertain initial blankholder force settings, friction variations, and blank placement errors. In this paper, the work is extended to include material property changes and thickness variations, both of which require a scaling of the optimal trajectory based on simple process mechanics. The work is then extended to include nonsymmetric parts, in particular a square dish-shaped part with corners of unequal radii. Results from these experiments are essentially identical to the axisymmetric case, with a virtually complete elimination of common process disturbances on forming stability.

Introduction

Three-dimensional sheet forming is a highly productive process capable of forming complex shapes at high rates. However, this productivity comes at the expense of lengthy and costly tooling development. A primary element of this tooling is the "blankholder" which provides the in-plane tensile bias necessary to avoid buckling failure of the sheet caused by in-plane compressive strains. Blankholder design is complicated not only by the difficult contours involved, but also by the critical nature of sheet stability in such bi-axial strain conditions. As a result, sheet-forming production is often disrupted by tensile or compressive instabilities (tearing and wrinkling failures) caused by incorrect blankholder forces. Despite careful design and optimization, variations in lubrication, material properties, and blankholder wear can drive a process into an unstable region of operation. This paper treats the problem of sheet stability as a real-time process control problem. The objective is to keep the margins of process stability within acceptable limits even when the abovementioned disturbances occur.

The approach taken here is largely empirical, and is based on the concept of trajectory or signature following. In this method, two accessible measures of process performance (punch force and flange draw-in) are monitored during "optimal" forming conditions. In subsequent forming cycles, the process is forced to follow these trajectories, and the blankholder force is modulated to accomplish real-time tracking. The key issues become robustness of the scheme to the expected variations and the ability to apply the method to general processes. In earlier reports on this work (Lee and Hardt, 1986; Fenn and Hardt, 1990) the results were all from axisymmetric forming of identical parts. In this paper, the control method is extended to nonsymmetric parts (square boxes with unequal corner radii) and to different materials (wrt yield stress and UTS) and material thicknesses. It is again shown that through the use of real-time blankholder control, optimal forming results can be maintained despite severe process disturbances.

Background

Research into the stability of sheet metal forming has concentrated on topics such as material properties, circular grid strain analysis, forming limit diagrams, finite element analysis, strain path corrections, and shape analysis. Below is a brief review of studies involving tearing, buckling, and forming limits, concentrating on those of direct relevance to the conical cup geometry.

The frequently used forming limit diagram, developed by Goodwin (1968) and Keeler (1969), is a good indicator of the tearing strains in plane strain loading. For a given material, these diagrams are developed by using a hemispherical punch stretch test and plotting the circumferential and radial strains.

Contributed by the Production Engineering Division for publication in the JOURNAL OF ENGINEERING FOR INDUSTRY. Manuscript received Jan. 1990; revised July 1992. Associate Technical Editor: S. G. Kapoor.

Downloaded From: https://manufacturingscience.asmedigitalcollection.asme.org on 06/29/2019 Terms of Use: http://www.asme.org/about-asme/terms-of-use
Copyright © 1993 by ASME

Once the diagram is developed it can be applied, with circle grid strain analysis of the formed sheet metal part, to help analyze specific tearing problems in the press shop. While there are many sheet metal parts that retain a flange, it is assumed in this research that the flange will be trimmed. This implies that the large body of research into flange buckling, such as Senior (1956), Yu and Johnson (1982), and Yossifon and Tirosh (1985), is not directly applicable to this work. The critical buckling issue in this research focuses on the unsupported region. Unfortunately, this topic has not yet received as much attention.

Havranek (1975) did perform experiments on buckling in the unsupported region of conical cups. By measuring the circumferential and radial strains on the unsupported region, he discovered a wrinkling curve on the forming limit diagram. A limitation of the wrinkling limit criterion is that it cannot be used when there is considerable bulging. In addition, its practical use is not as straightforward as that of the forming limit diagram for analyzing tearing.

As a follow up to Havranek's research, Hobbs (1978) analyzed the stability of production sheet metal parts. By including the wrinkling curve in the forming limit diagram and using circle grid strain analysis, Hobbs reported alleviation of both buckling and tearing failures of sheet metal parts.

The maximum height to which a conical cup can be successfully formed under constant blankholder force conditions is well established (Yoshida and Hayashi, 1979; Havranek, 1977). Yoshida and Hayashi state that restraint conditions on the flange, such as a draw bead and blank size, have little influence on the maximum formed depth of a conical cup. Typical height limits for a conical cup geometry and constant blankholder force are shown in Fig. 1. However, production problems often occur not because the peak height is too low, but because the blankholder force does not take advantage of the maximum possible height. The shape of the maximum height-blankholder force curve shown in Fig. 1 indicates that the optimum blankholder force changes substantially during process variations. Suboptimal heights will be achieved unless a blankholder control strategy can be found that can adjust the blankholder force as forming conditions change.

More recently there has been considerable work aimed at open-loop variation of the blankholder force to achieve higher failure limits in both cup drawing (e.g., Blümel et al., 1992) and large auto body panels (e.g., Kergen and Jodogne, 1992, and Hirose et al., 1990). This work implies that dynamic variation of the blankholder during the forming stroke can improve the forming characteristics, but does not prescribe any in-process means for determining the force trajectory.

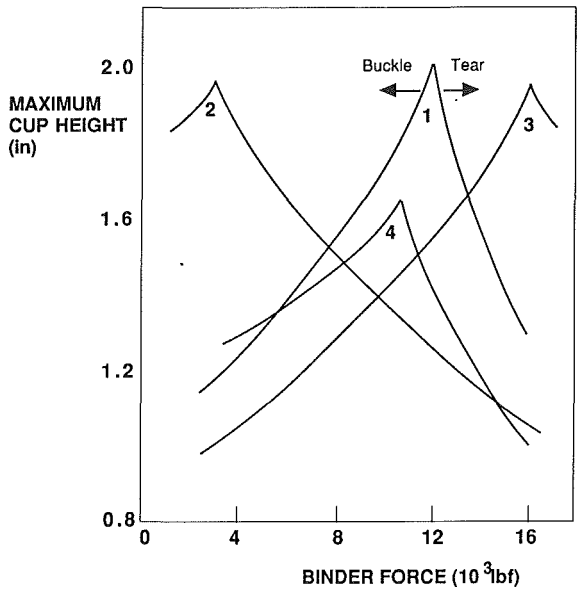

Fig. 1 Maximum formed height versus blankholder force (*Conical Cup Geometry*, from Havrenek (1975))

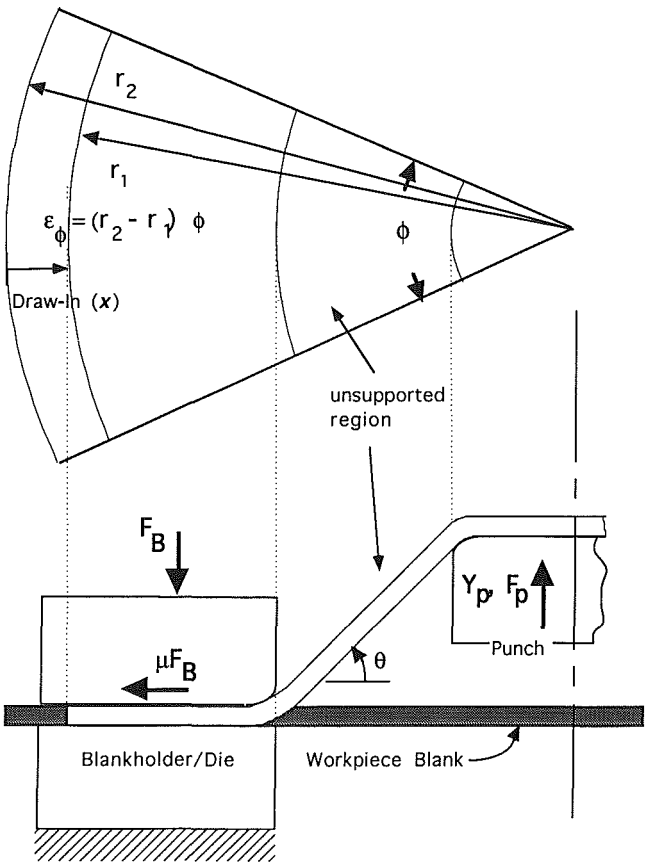

Fig. 2 Conical cup geometry and mechanics. The draw in (x) causes a circumferential strain ϵ_ϕ, which increases with radius.

Control Objectives

The key problem, as Fig. 1 illustrates, is the sharply defined optimum blankholder force for the conical cup. This implies that any perturbations that shift the optimum point will greatly reduce the maximum formed height before failure. The objective of the real-time control approach is to reduce this sensitivity by dynamically varying the blankholder force during the forming cycle to establish and maintain the optimum conditions for each cycle. To do so a measure of incipient failure must be available to use a feedback.

To develop such measures, it is necessary to briefly examine the mechanics of the conical cup test. As shown in Fig. 2 and Fig. 4(a), the process involves forming a frustum from an initially flat, circular blank. The wall of the frustum is "unsupported" during the stroke of the punch. As the material is drawn into this unsupported region from the flange, it develops a compressive circumferential strain, as illustrated in Fig. 2, which is at a maximum at the edge of the blank. Assuming that material is essentially "frozen" on the head of the punch (which has been verified by both experiment, Logan, 1986; Fenn, 1989, and by finite element simulation, Sim and Boyce, 1990), the maximum radial tensile stresses occur at the nose of the punch. Therefore one sees tearing failures at the nose of the punch, and buckling failure at the maximum radius in the *unsupported region*, which occurs at the die radius.

Tearing is caused by a localized necking instability and wrinkling is likewise a local buckling phenomenon. While some precursors of these failure modes are available (e.g., Thom-

Downloaded From: https://manufacturingscience.asmedigitalcollection.asme.org on 06/29/2019 Terms of Use: http://www.asme.org/about-asme/terms-of-use

ason, 1968, developed such a criterion for bulk deformation), it is not clear that any type of feasible measurement strategy would be applicable to direct detection of these phenomena.

Instead, the approach taken here is to develop approximate measures of the critical stress regions, and use these to regulate the process. The first case targets the critical tensile stresses. The tensile stresses at the nose of the punch are clearly related to the punch force and, more directly, to that force resolved along a tangent to the point of contact. Looking only at the neutral axis of the material, the radial stress σ_r is given by:

$$\sigma_r = \frac{F_T}{2\pi D_{punch} t}$$

where the *tangential force* F_T is given by:

$$F_T = \frac{F_p}{\sin(\theta)} \tag{1}$$

and F_p is the punch force, θ is the contact angle (which can be calculated from the punch displacement and the tooling geometry), D_{punch} is the punch diameter, and t is the material thickness (See Fig. 2). Thus, F_T is a measurable indication of the magnitude of the radial stress at the punch.

Given F_T, it is possible to construct a regulator to maintain a specified trajectory for this variable by continuously modulating the blankholder force F_B. Such a control scheme is shown in Fig. 3(*a*). However, the question remains as to what the correct target trajectory for F_T should be. The approach taken here is to determine the "optimal" value for F_B through constant blankholder force tests similar to those from Fig. 1. The corresponding trajectory for F_T is then recorded, and used to create an input trajectory for the F_T regulator. In this way, the blankholder force will be modified in response to lubrication, material, and thickness changes so as to maintain the desired F_T trajectory.

Note, however, that since F_T is an absolute measure of the tensile forces at the punch, its *optimal* trajectory will be changed significantly by changes in thickness, and by changes in yield and post-yield properties of the material. Accordingly, these effects must be explicitly accounted for, unless new trajectories are to be formulated for these changes. Such scaling methods are addressed later.

A second approach taken avoids some of these scaling problems. However, this approach is less solidly grounded in mechanics, and involves "flow control," whereby the process is controlled so as to maintain a specified amount of material in the free section at any time. This is accomplished by defining a *normalized average thickness* $\bar{t}$ in the unsupported area, given by:

$$\bar{t} = \frac{V_f}{A_f t_i} \tag{2}$$

where V_f is the volume of the frustum-shaped free section of the part, A_f is the surface area of frustum and t_i = initial thickness of material. Equation (2) is essentially the ratio of the volume actually in the free section to the volume necessary to maintain an average thickness equal to the initial blank thickness.

As forming progresses, the area will increase as a function of punch displacement, while the actual frustum volume can increase only if new material flows in from the blankholder. This flow can be measured by sensing the change in radius or circumference of the outer edge of the blank as it is drawn into the forming region. For the geometry shown in Fig. 2, $\bar{t}$ is given by:

$$\bar{t} = \frac{V_f}{A_t} = \frac{(D_d^2/4 + (D-x)x)}{D_p^2/4 + (D_p + D_d)^2/2} \tag{3}$$

where x is the displacement of the edge of the blank (the "draw-in"), D is the blank diameter, and D_p and D_d are the punch and die diameters, respectively. The calculation of $\bar{t}$ does not include the material flow into the frustum from the top of the punch because of "lock-up" over the punch early in the forming process. Flange swelling during draw-in is small and so the effect on $\bar{t}$ is also assumed to be negligible.

As with F_T, a regulator for $\bar{t}$ can be developed and used to track a desired trajectory, see Fig. 3(*b*). Again, this trajectory must be found empirically, but once determined, it should be independent of thickness changes, since Eq. (2) is scaled by thickness.

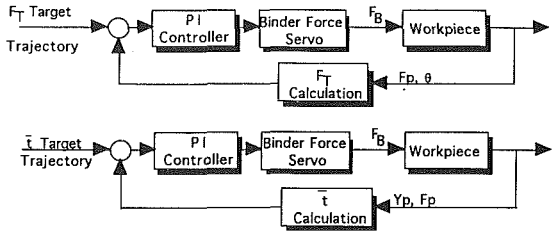

Fig. 3 Closed-loop stability controllers

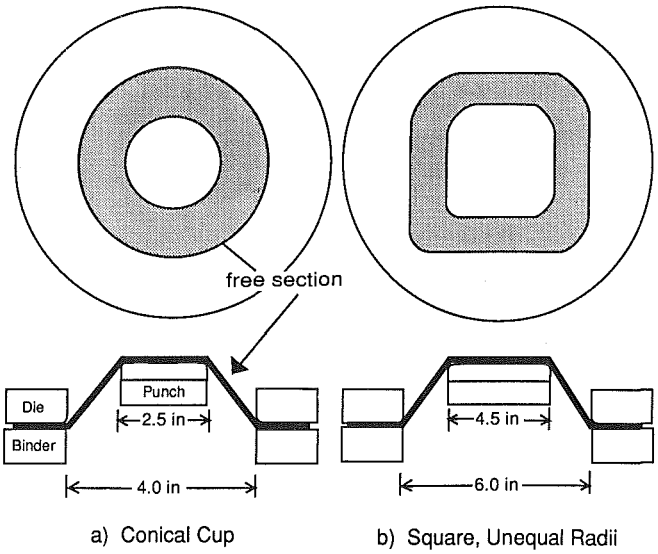

Fig. 4 Forming geometries used for experiments (nose radii for all tooling = 0.25 in corner radii for square punch = 0.5, 1.0, 1.25, 1.5 in for square die = 1.25, 1.75, 2.0, 2.25 in)

Experimental Methods

In all of the work presented here, two forming geometries are used (cf. Fig. 4). The first is a simple axisymmetric conical cup, as discussed in the above formulations. This forming geometry was chosen to emulate basic forming problems of unsupported material prior to complete closure of a die set. While the punch and die diameters and nose radii have a strong effect on the absolute values of formability test results, the dimensions shown in Fig. 4 were chosen after much experimentation to provide distinct tearing and/or buckling results. Likewise, the square geometry was chosen as a first step away from axisymmetry, and unequal corner radii were employed to create different strain conditions at each corner. The square pan sizing was done to create a free section of equal width to the conical geometry. Tests were also performed using a square die set with *equal* corner radii, but these results were so similar to the circular die set that they are not reported here. Detailed data for all these tests can be found in Fenn (1989).

Equipment. To perform the experiments detailed below,

Downloaded From: https://manufacturingscience.asmedigitalcollection.asme.org on 06/29/2019 Terms of Use: http://www.asme.org/about-asme/terms-of-use

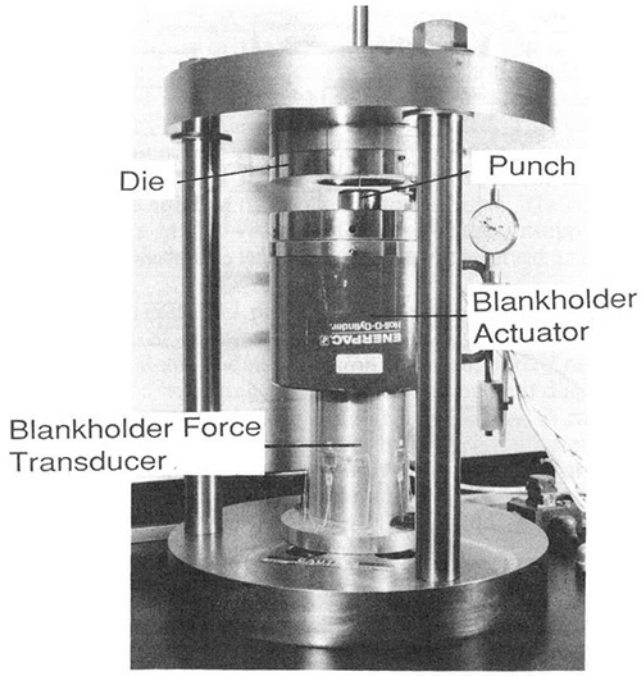

(a)

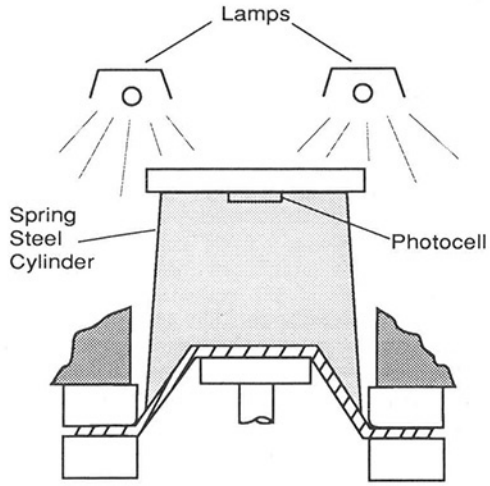

(b)

Fig. 5 Equipment for experiments (a) *forming press* (b) *buckling transducer*

a double-action servo-controlled forming process was developed by Lee and Hardt (1986). As shown in Fig. 5 it comprises a position-controlled hydraulic punch actuator and a force-controlled blankholder actuator. Each servo was implemented in analog hardware and tuned to have critically damped response with bandwidth in excess of 5 Hz. The dynamics of these servos are ignored in all the results, since the punch speed was slow (<2 in/min) enough as to render the tests quasi-static.

In addition to feedback measurements for the servos, several other measurements were available. The punch was instrumented for force to measure F_T, and the blankholder was equipped with an LVDT that could measure the displacement of the edge of the sheet (x) during draw-in. However, this latter method proved unreliable because of tearing of the sheet from anisotropic material and blankholder clearance variations. Accordingly, a method was devised that measured the circumferential contraction of the material, in effect averaging all draw-in over the entire circumference of the blank. This device comprised a lubricated string, anchored at one end, attached to an LVDT at the other, and then wound once around the periphery of the sheet.

Finally, to construct formability diagrams such as that shown in Fig. 1, it was necessary to detect failure quickly and accurately. Tearing failures were self-evident in the punch force, but buckling failures were very subtle. As discussed in Logan (1986) and Fenn (1989), buckling around the circumference of the conical cup was characterized by small amplitude "high frequency" variations in the radius. Typical amplitudes were on the order of 0.002 in. To detect such variations, and to reject small variations caused by anisotropy, a simple device was constructed, see Fig. 5(*b*). Comprising a cylinder made of thin spring steel of a diameter that caused it to rest near the bottom of the free section of the cup, the volume within the cylinder was sealed to light. The seal at the bottom was maintained, provided the cup remained round or slightly oval. However, as soon as high-frequency wrinkles appeared, the seal was broken, allowing light to enter the interior. By placing a photocell in the interior, this light could be detected, and a threshold set to denote a buckling failure. This device proved to be very accurate, and could even provide a signal that varied with the degree of buckling.

The basic scenario for all experiments (both open and closed-loop) was as follows: The blank material and the tooling were cleaned with a solvent, and then the lubricant in use was applied to the blank. The part was then centered in the die, and the blankholder closed to an initial force level. The basic forming cycle then proceeded and involved a constant punch velocity, with data from the transducers taken at constant punch displacement intervals.

Table 1 Standard conditions for forming trials

	CONICAL CUP	SQUARE PAN
High Friction	No lubricant	No lubricant
Standard Friction	STP/ SAE 20 Oil (1:3 mix)	DC 200 100 Centistoke silicone oil
Low Friction	Teflon Particle Spray	STP/ SAE 20 Oil (1:3 mix)

Optimal Trajectory Determination

To determine the trajectories for F_T and $\bar{t}$ at optimal forming conditions, a series of *constant blankholder force* experiments were performed. Each experiment involved forming a cup or square pan until failure by either tearing or buckling occurred. This was repeated for different values of F_B to develop a forming limit curve similar to that of Fig. 1. For these trials, a set of standard conditions were developed, as listed in Table 1. The blank diameter for the cup tests were chosen to give distinct buckling failures, and to confine the required blankholder forces to within the capacity of the process (0–60,000 lbs). The diameter of the pan blanks was scaled from the cup diameters to achieve geometrically similar flange lengths.

In subsequent experiments, changes from these conditions were introduced as process disturbances.

The results of constants F_B tests for both geometries are shown in Fig. 6. Note in both cases the clearly defined maximum punch height, and the corresponding optimal blankholder force.

It is important to distinguish between the two results, however, since the well-defined and easily quantified failure modes in the axisymmetric conical cup were not present in the square pan. Instead, it was apparent that tearing failure would (and did) occur at the nose of the smallest radius corner, and the buckling would occur not at the base of the corner radius, but

Downloaded From: https://manufacturingscience.asmedigitalcollection.asme.org on 06/29/2019 Terms of Use: http://www.asme.org/about-asme/terms-of-use

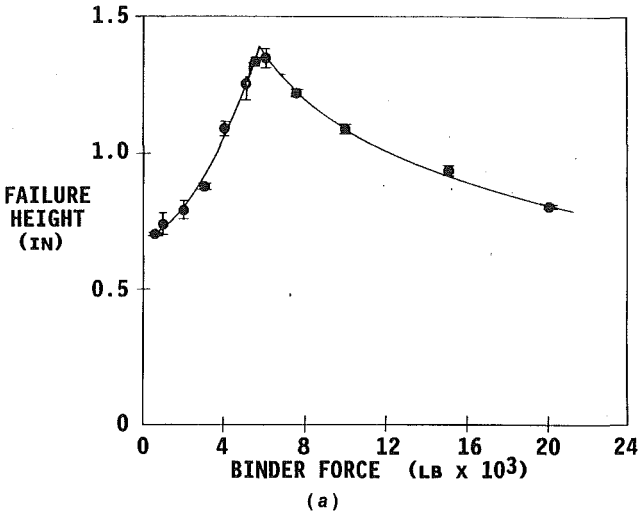

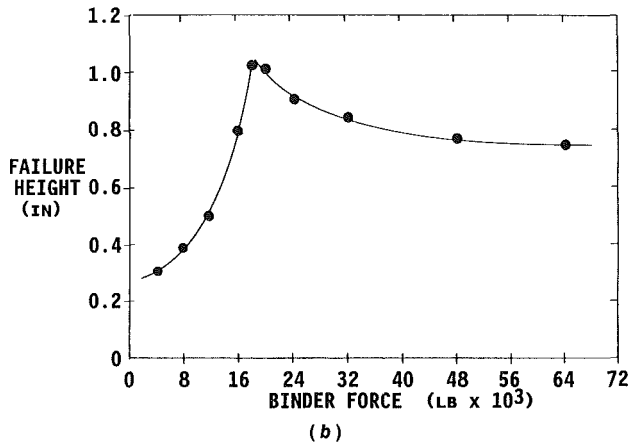

Fig. 6 Constant blankholder force results (standard conditions) (*a*) *conical cup* (*b*) *square pan*

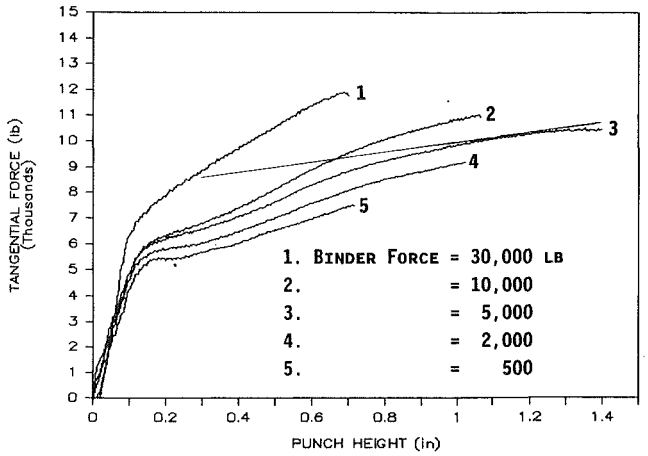

Fig. 7 F_T trajectories for the conical cup at various blankholder force levels

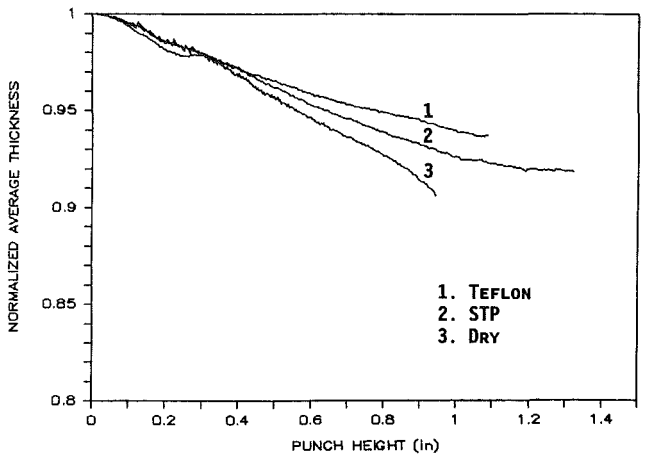

Fig. 8 $\bar{t}$ trajectories for the conical cup at various blankholder force levels

along the straight side between the two smallest radii. This can be explained heuristically as follows.

As is well-established from simple deep-drawing mechanics (Cook, 1965) the in-plane compression of the flange, caused by the shrinking circumference, will also cause a thickening of the flange. For the square pan, this thickening causes the majority of the blankholder traction to exist in the corner only, leaving the straight side effectively unrestrained. (Physical evidence to support this concept is the lack of burnishing of the straight portion of the flange and the greater draw-in in this region relative to the corners.) As a result, the circumferential compressive strains from the corners impinge on the straight wall, which is less restrained, and thus tend to buckle rather than to compress.

To create the target trajectories for both F_T and $\bar{t}$, it is first necessary to record the actual trajectory of these variables during forming. In Fig. 7, the F_T trajectories for various values of F_B during the conical cup test are shown. The optimal trajectory is clearly shown by the large punch height at the end. Note that each F_T trajectory has a distinct elastic region, quickly followed by a nonlinear region caused by plastic deformation and geometry effects, and then a nearly linear region up to failure. While it is conceivable that this exact curve could be recorded and then used as the input to the F_T control system, it was instead approximated by a straight line, as shown in the figure, to facilitate later scaling for off-nominal conditions.

In Fig. 8, the corresponding trajectories for $\bar{t}$ are shown, and here it is evident that the material is undergoing some net thinning even under optimal conditions. This can be expected, since stretching is necessary even when material flows in from the blankholder, to avoid wrinkling. For this curve, a simple exponential decay was used to approximate the trajectory.

When similar trajectories were examined for the square pan geometry, the same essential features were observed for both for F_T and $\bar{t}$, and again, linear and exponential curves were used to approximate the optimal trajectories.

Closed-Loop Blankholder Control Results

Tangential Force Control. The tangential force tracking system shown in Fig. 3 was used in a series of forming trials for both the conical cup and the square pan geometry. The actual operation of the control loop entailed starting at a *constant* blankholder force (the "initial blankholder force") and holding this value until the punch displacement reached a specified level.[1] This was necessary to allow the highly non-linear initial deformation to occur in a uniform manner, and because the trajectory approximations are only valid for later stages of displacement.

[1]The values used for all experiments was $Y_p = 0.3$ in. This value was chosen by conducting a series of experiment where this starting height was varied and the effect on final height was noted. It was found that the process is nearly insensitive to this starting value until it approaches 50 percent of the total deformation. Then the maximum height is rapidly diminished.

Downloaded From: https://manufacturingscience.asmedigitalcollection.asme.org on 06/29/2019 Terms of Use: http://www.asme.org/about-asme/terms-of-use

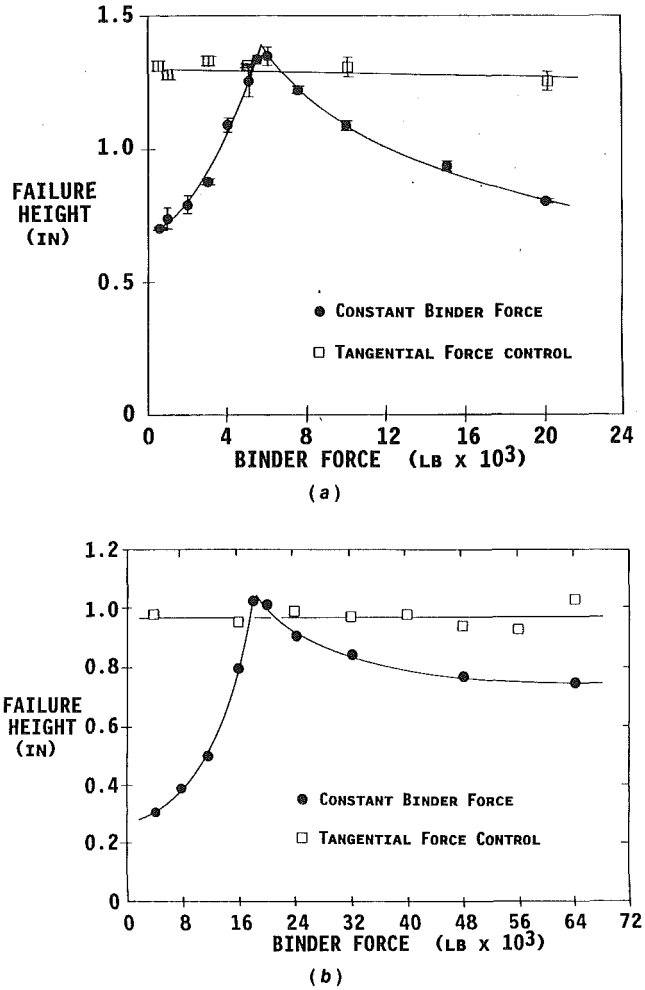

Fig. 9 Closed-loop F_T control (standard conditions) (*a*) *conical cup* (*b*) *square pan*

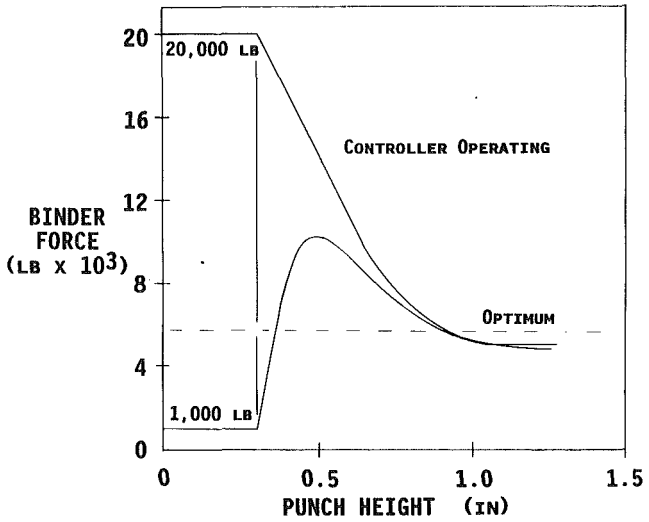

Fig. 10 Blankholder forces response for closed loop F_T control (*conical cup*, standard conditions)

Table 2 Lubricants used for forming tests

	CONICAL CUP	SQUARE PAN
Material	σ_Y = 36 ksi, UTS = 51 ksi	σ_Y = 29 ksi, UTS = 47 ksi
Thickness (in)	0.020	0.025
Diameter (in)	6.25	9.08
Lubricant	STP SAE 20 Oil, 1:3 mix	100 Centistoke Silicone Oil
Eccentricity (in)	0	0

The results for the standard conditions for the two geometries are shown in Fig. 9 along with the constant force test results of Fig. 7. Note that on this plot at the abscissa is the *initial* blankholder force for the closed-loop results, and the actual blankholder force of the constant blankholder force tests. Three tests were run for each initial blankholder force level, as indicated by the range bars on the figure.

Both these results demonstrate that the control system has effectively moved from the initial force "estimate" to a force that permits the optimal punch height to be reached. As a result, the control system has effectively desensitized the process to initial blankholder force estimates. The actual blankholder force during forming undergoes a transient, and then settles to near the optimum level as Fig. 10 shows. The apparent process dynamics here are actually the result of the punch speed-dependent material flow for this process. While the control system modulates the blankholder force, the reflection of this force to the punch depends upon continued travel of the punch, and the "response" of the punch force to blankholder force changes is thus a function of the punch travel *and* the radial strain of the material.

Process Disturbances: Lubrication. The most prevalent and insidious process disturbance is a change in the state of friction in the tooling. While the use of draw beads may mitigate some of these effects, it is nonetheless a dominant problem (Siekirk, 1986). With a simple flat blankholder, such as used here, the effect of lubrication and the attendant change in friction conditions have the obvious effect of changing the blankholder force-tangential force relationship. Clearly, one of the most important goals of closed-loop blankholder control is to eliminate process sensitivity to lubrication changes.

Accordingly, the same protocol as used for "standard conditions" was repeated for both geometries, but with two extreme lubrication conditions, as Table 2 lists. Different lubricants were used for the square pan because this geometry required considerably higher blankholder forces than did the cup. In fact, although dry conditions were used, they were found to yield *lower* effective friction coefficients than the silicon oil, and when dry tooling was used, considerable chatter became evident. Consequently, no "low-friction" control tests were performed for the square pan.

Since the change in lubrication would shift the optimum blankholder force, a constant blankholder force test was also performed for each lubrication condition for comparison to the closed-loop tests. However, the target F_T trajectories were not altered in any way, thus the closed-loop experiments examined the ability of the control scheme to deal with a totally unexpected disturbance.

The results for the low friction conditions are shown in Fig. 11, and the high friction conditions for the cup are shown in Fig. 12. Note that in both cases the optimum values have shifted significantly from those in Fig. 8, but the control system has again completely eliminated the effect of uncertainty and formed to the optimum height in all three cases. However, it is important to note here that the control system does not (and indeed cannot) force the maximum formed height to a level higher than is achievable with that lubrication. Thus, a severe change in lubrication (as seen in the "dry" case) will affect the maximum possible formed height, but the control system will always produce that height, regardless of prior knowledge about optimum blankholder force levels.

Downloaded From: https://manufacturingscience.asmedigitalcollection.asme.org on 06/29/2019 Terms of Use: http://www.asme.org/about-asme/terms-of-use

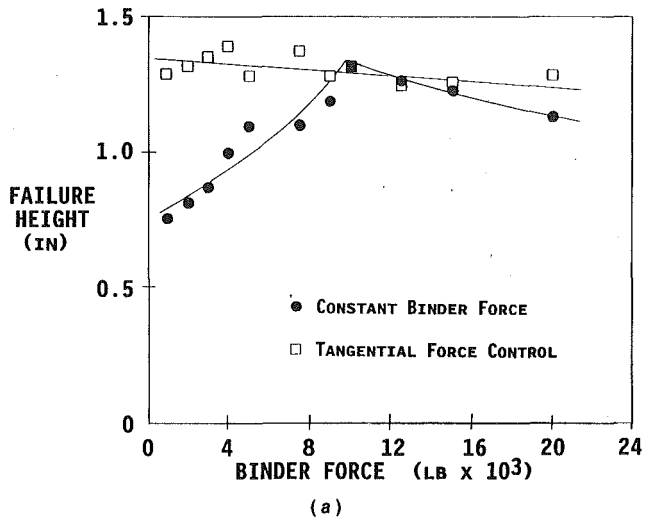

(a)

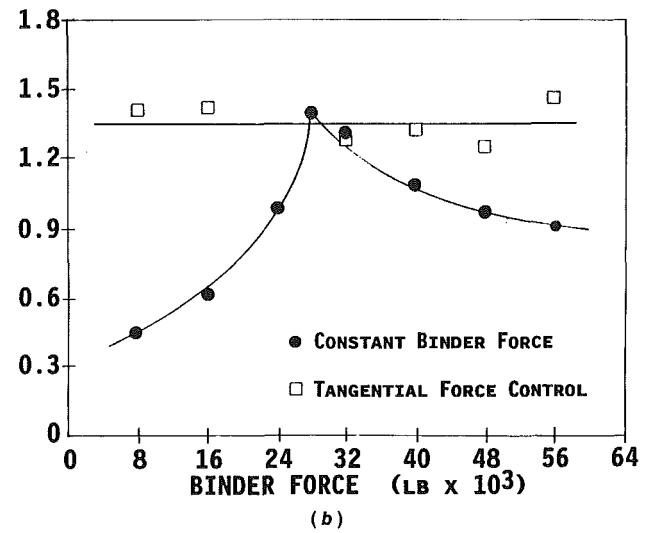

(b)

Fig. 11 Closed-loop F_T control (low friction) (*a*) *conical cup* (*b*) *square pan*

Process Disturbances: Material Changes. Disturbances related to the blank material itself, specifically changes in intrinsic properties (yield point, flow stress) and extrinsic properties (thickness) are the most difficult to respond to since they shift both the optimal force and the corresponding blankholder force. These disturbances combine to change entirely the way in which the material forms and its propensity for tearing and for buckling; and with regard to the F_T strategy, change the optimal target trajectory significantly. However, the objective here is to develop a controller that can respond to these changes without the need to completely "re-tune" the system.

From the perspective of the F_T trajectory, it is clear that an increased material thickness will increase F_T at failure, because of the greater stress-carrying area at the punch. A material with higher UTS will also increase F_T at failure. However, it is not easy to determine at what punch height this failure will occur, since the increased thickness will also change the buckling propensity. To address this problem while avoiding empirically creating F_T trajectories for each new material (which is in fact a time-intensive activity), a *scaling* of the standard F_T trajectory was developed based on a simple model of the conical cup mechanics. This model (see Fenn, 1989, for details) first scales the F_T target trajectory vertically by the ratio of the material thickness to the standard so as to maintain equal stress at failure:

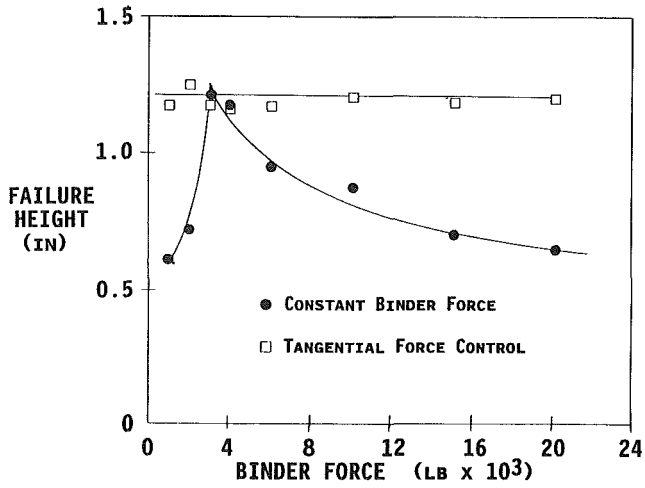

Fig. 12 Closed-loop F_T control (high friction) conical cup

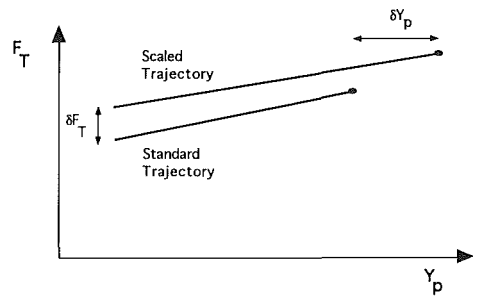

Fig. 13 F_T target scaling for material thickness change

$$\delta F_T^{max} = \frac{t}{t_{standard}} \tag{4}$$

While this accounts for the higher stress at failure, the new target must likewise be scaled horizontally. As shown in Fenn (1989), this scaling can be done on the basis of simple plastic buckling theory. The result is that the terminal punch displacement is changed according to:

$$\delta Y_p = \left(\frac{t}{t_{standard}}\right)^{1.25} \tag{5}$$

The changes to the "standard" target line are shown in Fig. 13.

To examine the use of this scaling, a set of experiments were performed using a material with different thickness from the standard material of Table 1 (0.025 in. versus 0.020 in.) and a similar UTS (49 ksi versus 47 ksi). The experiments were identical to those performed above, and the target line was scaled according to Eqs. (2) and (3). Thus, the target *line* was scaled 25 percent vertically and the *endpoint* horizontally by 32 percent ($1.25^{1.25}$). The results of this test are shown in Fig. 14, and it is evident that this scaling has again permitted the F_T control to reach the true optimum for the new material.[2]

As for intrinsic material properties, many factors can change, most importantly the strength and ductility of the material. However, since the F_T controller is stress-based, the ultimate tensile strength (UTS) is used as the prime constitutive parameter. Scaling for UTS presents essentially the same problem as

[2]It is interesting to note that if a thicker material than standard is used, and no scaling is applied, the F_T control will still allow the optimum height of the thinner material be reached, since it is lower than the true optimum for the thick material. While this suggests some robustness in the controller, the reverse situation of a thinner one expected material would confound the controller and cause premature failure.

Downloaded From: https://manufacturingscience.asmedigitalcollection.asme.org on 06/29/2019 Terms of Use: http://www.asme.org/about-asme/terms-of-use

thickness, except that no impact on buckling threshold is assumed, since this effect is primarily elastic and thus affected only by thickness changes. Unfortunately, no test material was available to perturb only the UTS, but a combined thickness and UTS change were made for the square pan geometry. The effect of this change, applying the above scaling to the "standard" target line of closed-loop F_T control, is shown in Fig. 15. The thickness was again changed from 0.020 in. to 0.025 in. and the UTS increased from 47 to 65 ksi. Again, in comparison with the constant force tests, it is clear that the optimum failure height has been achieved.

The other process variations examined were blank offset (eccentric by 0.2 in.) and blank diameter (increase of 4 percent). Both of these changes were shown to affect the location of the optimum blankholder force, and eccentricity had a significant effect on optimum failure height. In both cases, and for both geometries, the F_T controller completely compensated for this effect.

Control Using $\bar{t}$. A similar set of experiments were performed using the $\bar{t}$ control scheme instead of the F_T approach. The same standard and perturbed conditions as above were used, but most tests were confined to the conical cup geometry.

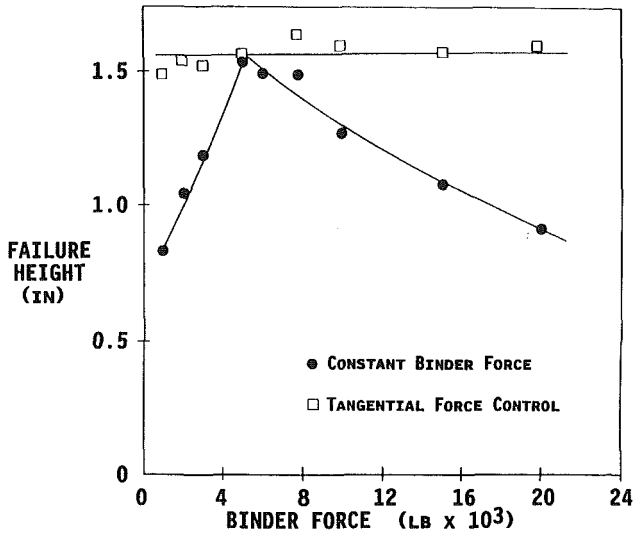

Fig. 14 Effect of thickness change from standard conditions (*Conical Cup*, F_T control) thickness = 0.025 in.

The standard test results for both geometries is shown in Fig. 16. Again, the use of various initial blankholder force estimates caused the controller to modulate the blankholder force and eventually achieve near optimum value before failure (see Fig. 17).

It is interesting to note that in addition to having brought the blankholder force to the optimum value for standard conditions, the $\bar{t}$ controller also brought the corresponding F_T trajectories to nearly identical values, as shown in Fig. 18. Thus it appears that both schemes have similar responses, and in fact the main difference is in the means and practicality of application.

Effect of Process Disturbances. The $\bar{t}$ control scheme was subjected to the same set of process disturbances as above, including lubrication, diameters, offset, thickness, and UTS changes. As expected, the first three were easily accommodated by the controller. The more important issue is the effect of the inherent thickness scaling and the apparent independence of the $\bar{t}$ measure on material properties.

The effect of thickness was investigated, as before, by increasing thickness to 0.025 in., but no scaling of the target $\bar{t}$ was used. As Fig. 19 shows, the controller nearly reached the optimum values, but was consistently lower than the true optimum. The use of a scaled target for F_T control achieved slightly better performance, but when no scaling was used, the F_T control was consistently 20 percent below the true optimum. Thus, the $\bar{t}$ control exhibits greater robustness to thickness changes, as could be expected from its structure.

When the UTS alone was changed from 47 to 58 ksi (Fig. 20), the performance was less desirable. While at lower initial blankholder forces the controller gave optimal heights, as the initial force increased, the height consistently decreased. This may be attributable to the slow response of the controller, which had difficulty reaching the optimum F_B before tearing failures occurred.

Discussion and Conclusions

The basic closed-loop blankholder control methods investigated here have been shown to force the process to near optimal conditions even when significant process disturbances occur. While lubrication and blank diameter changes can be accommodate with no *a priori* knowledge of the disturbance, the same is not true of material changes. For these, the change must be known if optimal conditions *for that new material* are desired. However, given knowledge of the material UTS and

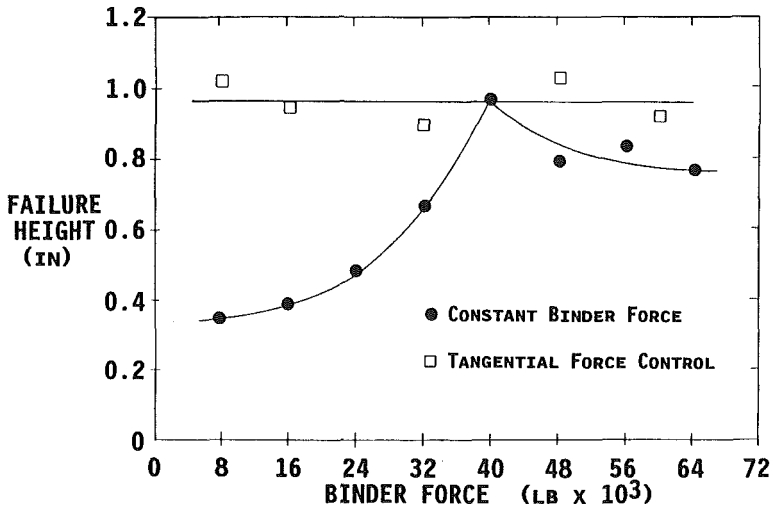

Fig. 15 Effect of combined thickness and UTS perturbations using target scaling. (F_T control, *square pan* geometry)

Downloaded From: https://manufacturingscience.asmedigitalcollection.asme.org on 06/29/2019 Terms of Use: http://www.asme.org/about-asme/terms-of-use

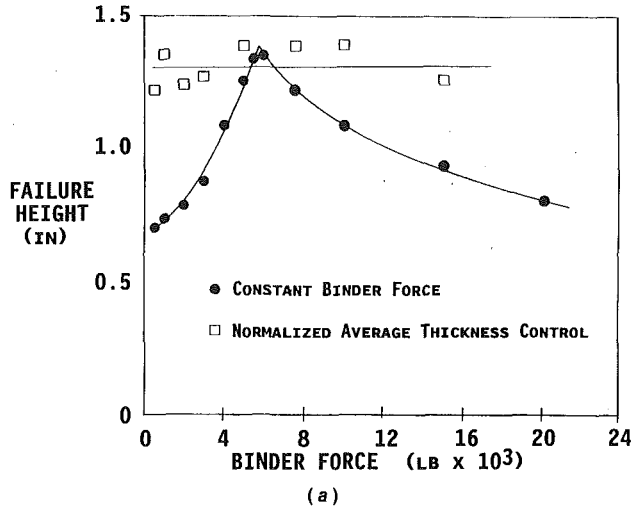

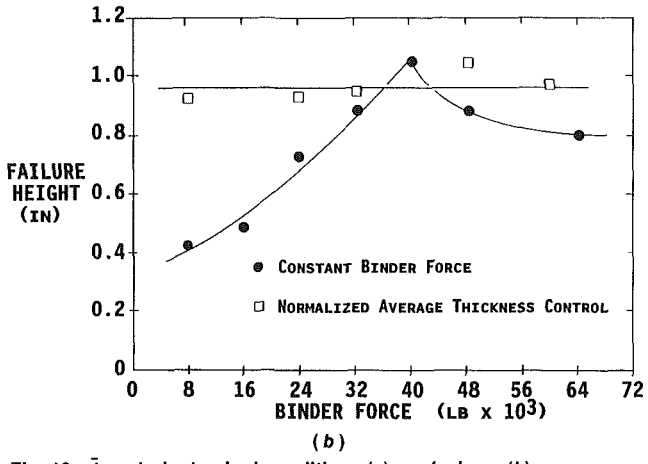

Fig. 16 $\bar{t}$ control, standard conditions (*a*) *conical cup* (*b*) *square pan*

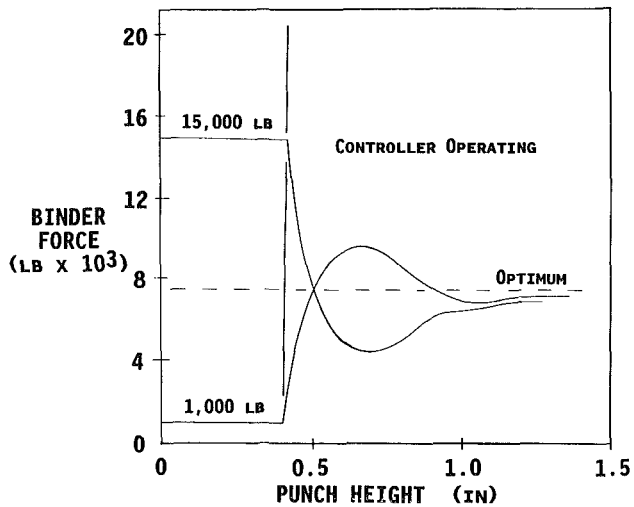

Fig. 17 Blankholder force trajectories during the $\bar{t}$ control test of Fig. 16, *Conical Geometry*

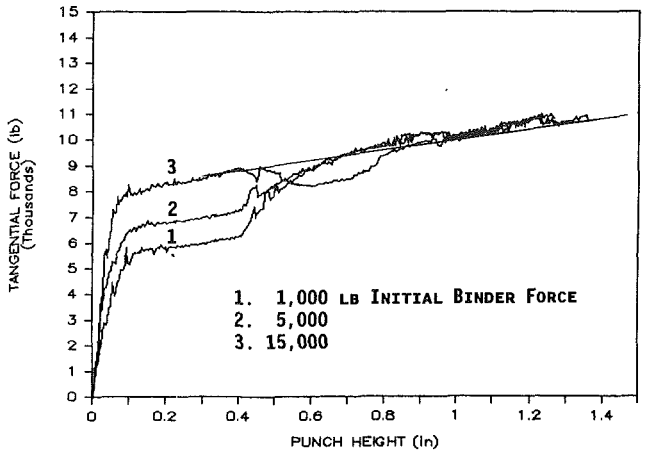

Fig. 18 Tangential force trajectories during the $\bar{t}$ control test of Fig. 16 (*Conical Geometry*)

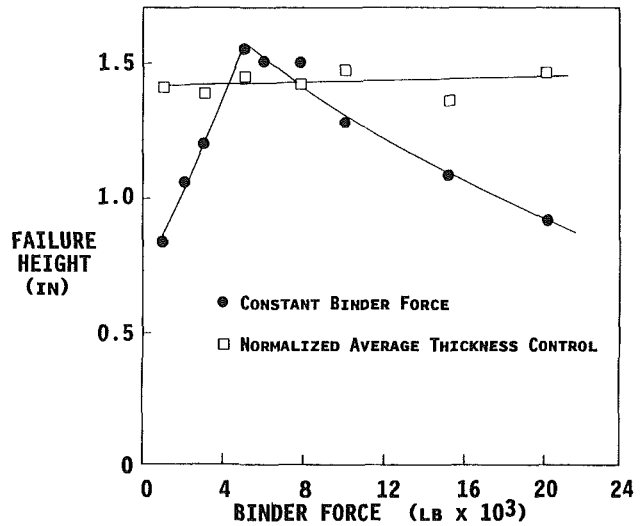

Fig. 19 Effect of a thickness changes on $\bar{t}$ controller performance (*Conical Cup*, thickness = 0.025 in.)

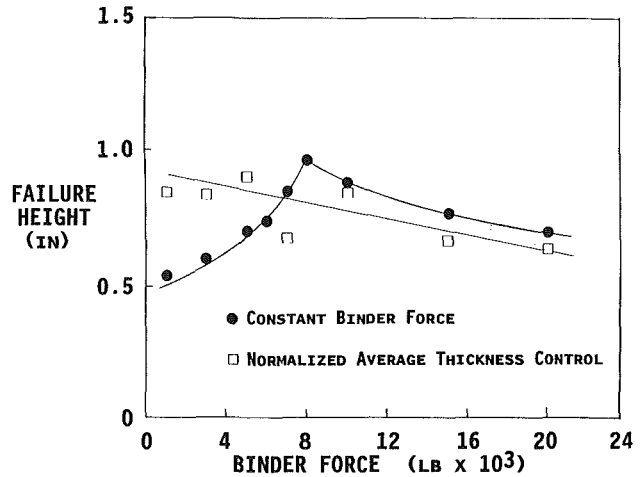

Fig. 20 Effect of a UTS change on $\bar{t}$ controller performance (*Conical Cup*, UTS = 58 ksi)

thickness, a scaling scheme based on equal stress and buckling levels has been proposed which obviates retesting the material to determine a new optimum target line.

Both the F_T and $\bar{t}$ control methods work well, with the latter showing greater robustness to *unknown* thickness changes. Within these experiments, the F_T approach requires simpler instrumentation, which implies easier implementation on full scale processes. However, it is not clear that gross punch force will reflect local failure conditions for large complex parts. Instead, a local draw-in measurement and a modified $\bar{t}$ strategy may work best.

It is quite apparent from this work that even simple control strategies to modulate blankholder forces in real-time can sig-

Downloaded From: https://manufacturingscience.asmedigitalcollection.asme.org on 06/29/2019 Terms of Use: http://www.asme.org/about-asme/terms-of-use

nificantly affect the maintenance of consistent performance of sheet-stamping operations. These methods can be refined through further empirical and numerical investigation, and Boyce and Sim (1990), in collaboration with the authors, have pursued the latter. Their investigation has confirmed the results presented here, and reinforces the notion that while the F_T approach does relate to a critical stress state, the $\bar{t}$ method is based more on a convenient, measurable, and consistent trajectory that reflects the forming state (as suggested by Fig. 18).

One aspect of this research that has not been fully explored is the use of active blankholder control to actually *extend* the forming limits for a given geometry. As suggested by Boyce and Sim (1990) and Hirose et al. (1990), it may be possible to prevent local necking and to distribute more evenly the stretching strains control by dynamic variations of the blankholder force during the latter stages of forming.

The move from axisymmetric cones to unequal radii pans demonstrated the ability to extend this algorithm even when failure sites were highly localized. The motivation behind such a test was that with arbitrary geometries and part scales, failure sites would also be localized, and that application of this might best be performed near that site (using a local draw-in measurement) rather than by continuing with the global scheme used here.

All experiments and analysis performed here employed a flat blankholder, relying on friction for the restraining force. In many tooling applications this provides insufficient restraint, and draw beads are added. These operate by effectively forcing the material through a series of local bends, and the force is modulated not by a normal force, but rather by a displacement that modulates the bending strains in the bead. While it requires further investigation, it is expected that a substitution of blankholder displacement for force can be made when draw beads are present, and similar results will be obtained.

Acknowledgment

This work was supported by General Motors Corporation, and the assistance of Dr. Robin Stevenson is gratefully acknowledged.

References

Blümel, K., Frings, A., and Hartmann, G., 1992, "Shearing and Stamping Hot-Rolled Material," *Autobody Stamping Applications an Analysis*, SAE SP-897, pp. 41–49.

Boyce, M., and Sim, H., 1990, "A Finite Element Analysis of Real-Time Sheet Forming Stability Control in Cup-Forming," ASME *Journal of Engineering Materials and Technology*.

Cook, N. H., 1965, *Analysis of Manufacturing Processes*, McGraw-Hill, New York.

Fenn, R. C., 1989, "Closed-Loop Control of Forming Stability During Metal Stamping," Ph.D. Thesis, Massachusetts Institute of Technology, Aug.

Fenn, R. C., and Hardt, D. E., 1990, "Real-Time Sheet Forming Stability Control," *Proc. International Deep Draw Research Group*, June.

Havranek, J., 1977, "The Effect of Mechanical Properties of Sheet Steels on the Wrinkling Behaviour During Deep Drawing of Conical Shells," *Journal of Mechanical Working Technology*, Vol. 1, No. 2, November, pp. 115–129.

Havranek, J., 1975, "Wrinkling Limit of Tapered Pressings," *Journal of the Australian Institute of Metals*, Vol. 20, No. 2, June, pp. 114–119.

Hirose, Y., Hishida, Y., Furubayashi, T., Oshima, M., and Ujihara, S., 1990, "Techniques for Controlling Wrinkles by Controlling the Blank Holding Force, Part 1," *Proc. 4th Symposium of the Japanese Society for the Technology of Plasticity*.

Hirose, Y., Hishida, Y., Furubayashi, T., Oshima, M., and Ujihara, S., 1990, "Application of BHF-Controlled Forming Techniques, Part 2," *Proc. 4th Symposium of the Japanese Society for the Technology of Plasticity*.

Hobbs, R. M., 1978, "Use of Grid Strain Analysis for Die Development and Process Control in Australian Press Shops," *Sheet Metal Industries*, Vol. 55, April, pp. 451–464.

Kergen, R., and Jodogne, P., 1992, "Computerized Control of the Blankholder Pressure on Deep Drawing Processes," *Autobody Stamping Applications an Analysis*, SAE SP-897, pp. 51–56.

Lee, C., and Hardt, D. E., 1986, "Closed-Loop Control of Sheet Metal Stability During Stamping," *1986 North American Manufacturing Research Conference*, May 28–30.

Lee, C. Y., 1986, "Closed-Loop Control of Sheet Metal Stability During Forming," S.M. Thesis, Massachusetts Institute of Technology, Feb. 1986.

Logan, R. W., 1985, "Sheet Metal Formability Simulation and Experiment," Ph.D. Thesis, University of Michigan.

Meyers, M. A., and Chawla, K. K., 1984, *Mechanical Metallurgy Principles and Application*, Prentice Hall, Englewood Cliffs, NJ, pp. 625–641.

Senior, B. W., 1956, "Flange Wrinkling in Deep-Drawing Operations," *Journal of the Mechanics and Physics of Solids*, Vol. 4, pp. 235–246.

Tesawa, K., and Nishimura, G., 1931, *J. Soc. Naval Arch.*, Vol. 47, p. 129.

Yoshida, K., and Hayashi, Y., 1979, "Developments in Research into Sheet Metal Forming Processes in Japan—Part 2," *Sheet Metal Industries*, Vol. 56, March, pp. 261–270.

Yossifon, S., and Tirosh, J., 1985, "Buckling Prevention by Lateral Fluid Pressure in Deep-Drawing," *Int. J. Mech. Sci.*, Vol. 27, No. 3, pp. 177–185.

Yu, T. X., and Johnson, W., 1982, "The Buckling of Annular Plates in Relation to the Deep-Drawing Process," *Int. J. Mech. Sci.*, Vol. 24, No. 3, pp. 175–188.

Downloaded From: https://manufacturingscience.asmedigitalcollection.asme.org on 06/29/2019 Terms of Use: http://www.asme.org/about-asme/terms-of-use